JOURNAL OF SOLID STATE CHEMISTRY 120, 137–145 (1995)

Intercalated Vanadyl Vanadate $(V^{IV}O)[V^{V}O_4] \cdot 0.5[C_3N_2H_{12}]$: Hydrothermal Synthesis, Crystal Structure, and Structural Correlations with V_2O_5 and Other Vanadyl Compounds

Didier Riou and Gérard Férey[1]

Laboratoire des Fluorures, URA CNRS 449, Faculté des Sciences, Université du Maine, Avenue Olivier Messiaen, 72017, Le Mans Cedex, France

Received June 19, 1995; accepted June 22, 1995

$(VO)[VO_4] \cdot 0.5[C_3N_2H_{12}]$ is an intercalated vanadyl vanadate. It has been hydrothermally synthesized (453 K, 24 hr autogeneous pressure) from a mixture of V_2O_5, SiO_2, HF, 1,3-diaminopropane, and H_2O in the ratio 1:2:2:0.6:80. It is monoclinic (space group $P2_1/n$ (no. 14)) with $a = 7.999(1)$ Å, $b = 10.008(1)$ Å, $c = 15.703(1)$ Å. $\beta = 100.49(1)°$, $V = 1236.2(2)$ Å^3, and $Z = 8$. The structure, refined to $wR_2 = 0.066$, $R = 0.029$, is two-dimensional, with protonated amines inserted between the inorganic layers. The latter are compared to other layered compounds containing vanadyl ions. Structural correlations as well as possible forms of deintercalation of the title compound are discussed.

INTRODUCTION

Several years ago, Kessler and co-workers (1–4) developed a new route of synthesis in the presence of fluorine. The addition of this element favors mineralization and induces crystallization at neutral or acidic pH. Moreover, fluorine is often incorporated to the open frameworks and leads to new topologies.

Recently (5–15), we focused attention on the synthesis of a new series, labeled ULM-*n* of fluorinated alumino- and gallophosphates in the systems M_2O_3 (M = Al, Ga)–P_2O_5–HF–template–H_2O. In these phases, the situation of fluorine is different since it is directly involved in the coordination sphere of M. We recently inferred that the particularly strong interaction between amino groups and the fluorine contained in the secondary building units of the structure led to ion pairs whose geometric characteristics induce the observed structures. In such a context, other metallic ions of Al and Ga may lead to microporous compounds. Simultaneously with Sogomanian *et al.* (16, 17), we found evidence for microporous solids with vanadium, containing fluorine or not (18, 19), and more recently, compounds with iron (20, 21). In an attempt to synthesize vanadium silicates, we obtained large crystals of a new phase whose structure is described here.

EXPERIMENTAL

Synthesis

The title compound was prepared by hydrothermal synthesis under autogeneous pressure. The reactants were vanadium oxide (V_2O_5; Aldrich, 99.6%+), silica (SiO_2, Prolabo RP Normapur), hydrofluoric acid (40% HF Prolabo RP Normapur), and 1,3-diaminopropane $C_3H_{10}N_2$ (Aldrich; 99%+). The starting mixture corresponding to the molar composition 1 V_2O_5, 2 SiO_2, 2 HF, 0.6 amine, and 80 H_2O was placed without stirring in a Teflon-lined stainless steel autoclave, heated at 453 K for 24 hr, and then cooled to room temperature for 24 hr. The pH of the synthesis increased from 4 before heating to 5 at the end of the reaction. The final mixture contained two phases: unreacted powdered silica and numerous dark-green, hexagonal plate single crystals. They were filtered off, washed with distilled water, and dried at room temperature. Chemical analysis of the dark crystals showed that the solid did not contain any silicon and fluorine atoms. The analysis of vanadium by a solution of Fe^{2+} (for V^{5+}) and of MnO_4^- (for V^{4+}) revealed the existence of both V^{5+} and V^{4+} in the compound with a 1:1 ratio (V^{5+} exp: 22%; V^{4+} exp: 24%) and a content corresponding to the formula V_2O_5, 0.5 1,3-diaminopropane, hereafter denoted $(VO)VO_4 \cdot 0.5$ DAP (V^{5+} calc: 23.2%; V^{4+} calc: 23.2%). Magnetic susceptibility measurements were obtained from a Faraday balance between 4 and 300 K.

Structure Determination

The quality of the prismatic-shaped single crystal was tested by optical observation and Laue photographs. Intensity data collection was performed with a Siemens AED-2 four-circle diffractometer with conditions of data collection summarized in Table 1 and which led to the description of the structure with the space group $P2_1/n$ (no. 14). The data were corrected for Lorentz-polarization and absorption effects. The scattering factors and anomalous dispersion corrections were taken from the International Tables

0022-4596/95 $12.00

TABLE 1

Crystal Data and Details of the X-Ray Data Collection of $[VO(VO_4)] \cdot 0.5\ C_3N_2H_{12}$

Empirical formula/formula weight:	$V_4O_{10} \cdot (N_2C_3H_{12})$/440 g
Determination of cell parameters	32 reflections ($28° \leq 2\theta \leq 32°$)
Space group	$P2_1/n$ (no. 14)
Cell dimensions	a = 7.999(1) Å
	b = 10.008(1) Å β = 100.49(1)°
	c = 15.703(1) Å
Volume/Z	V = 1236.2(2) Å^3 Z = 4
Density (calculated)	2.364 g · cm^{-3}
Wavelength/monochromator	0.71069 Å (Mo$K\alpha$)/graphite
Temperature	293 K
Scan mode	ω–θ
Step scan	$37 \leq N \leq 42$, every 0.035° and 4 sec
Aperture	3 × 3 mm^2
Absorption coefficient	3.155 mm^{-1}
Absorption correction	Gaussian method
Transmission factors	T_{min} = 0.541 T_{max} = 0.917
F(000)	864
Crystal size	0.015 × 0.180 × 0.180 × 0.228 mm
Natural faces	{001} × {22 − 1} × {−221} × {010}
Angular range of data collection	$5° \leq 2\theta \leq 70°$
Range of measured h, k, l	$-12 \leq h \leq 12$; $0 \leq k \leq 16$; $0 \leq l \leq 25$
Standard reflections (3)	(7 − 17); (−2 − 9 − 2); (292)
Measured every	60 mn
Maximum intensity variation	2%
Measured reflections	6512
Independent ref. ($I > 2\sigma(I)$)	3165 [R(int) = 0.026]
Number of refined parameters	176
Extinction coefficient	0.0002(2)
Weighting scheme	$1/[\sigma^2(F^2) + (0.0312\ P)^2) + 0.51P]^a$
Final Fourier residuals	−0.41 to 0.57 $e^- \cdot$ Å^{-3}
Goodness-of-fit on $F2$	1.053
Final R indices ($I > 2\sigma(I)$)	R_1 = 0.0294, wR_2 = 0.0658[a]

[a] As defined in (24).

for X-Ray Crystallography (22). The structure was solved by using the direct method analysis of the SHELXS-86 program (23). Vanadium atoms were located first. The anions of the matrix were then found by difference Fourier maps. Refinement was performed by full-matrix least-squares analysis of SHELXL-93 (24). At this stage of the refinement, the hydrogen atoms became visible. The refinement with anisotropic thermal parameters for V, O, C, N, and isotropic parameters for H gives wR_2 = 0.066 and R = 0.029.

The atomic coordinates with isotropic thermal parameters and selected bond distances and angles are listed in Tables 2 and 3, respectively. Table 4 provides the valence bond analysis (25) of the compound. The list of U_{ij} and of structure factors can be obtained on request to the authors.

DESCRIPTION OF THE STRUCTURE

This structure (Fig. 1) corresponds to a two-dimensional compound, with organic and inorganic layers alternating along the c axis. In the inorganic sheet, the vanadium atoms, on four distinct crystallographic sites, exhibit two types of coordination polyhedra. V(1) and V(2) are in a square pyramid of oxygens, while V(3) and V(4) are tetrahedrally coordinated. As usually observed in the crystal chemistry of V^V and V^{IV}, the very short bonds [1.610 (V(1)), 1.612(V(2)), 1.653(V(3)), and 1.648 Å (V(4))] correspond to the V=O bond, which is terminal and points toward the organic layers. In the square pyramids, the other V–O bonds lie in the range 1.917–1.975 Å. In each tetrahedron, two other medium distances (1.695–1.717 Å) correspond to the vertex linkage with one square pyramid,

TABLE 2

Atomic Coordinates ($\times 10^5$ for V and 10^4 for the Other Atoms) and Equivalent Isotropic Factors ($\times 10^4$) in $VO(VO_4)\cdot 0.5[C_3N_2H_{12}]$

Atom	x	y	z	U_{eq} (Å^2)
V(1)	05767(5)	74225(4)	44365(2)	98(1)
V(2)	07197(5)	26251(4)	96000(2)	98(1)
V(3)	21310(5)	05545(4)	47248(3)	104(1)
V(4)	21339(5)	95262(4)	97209(3)	109(1)
O(1)	4103(2)	1229(2)	4998(1)	170(3)
O(2)	0357(3)	7143(2)	3413(1)	235(4)
O(3)	4040(2)	8736(2)	9907(1)	200(4)
O(4)	0957(2)	1121(2)	5462(1)	168(3)
O(5)	2571(2)	3734(2)	0236(1)	138(3)
O(6)	1266(3)	9365(2)	8691(1)	246(4)
O(7)	1281(3)	1005(2)	3727(1)	219(4)
O(8)	0872(2)	8822(2)	0375(1)	162(3)
O(9)	0671(3)	2914(2)	8586(1)	229(4)
O(10)	2474(2)	6303(2)	5022(1)	147(4)
N(1)	1573(3)	7742(3)	7308(2)	242(5)
N(2)	1561(3)	9220(3)	2355(2)	255(5)
C(1)	3636(4)	1346(3)	7397(2)	315(7)
C(2)	3241(4)	9078(3)	2102(2)	292(6)
C(3)	5369(4)	1153(4)	7120(2)	306(6)
H(1)	1600(34)	8300(3)	7751(4)	501(35)
H(2)	0704(17)	7951(9)	6889(12)	501(35)
H(3)	2540(17)	7806(7)	7106(16)	501(35)
H(4)	1259(17)	8444(8)	2559(17)	501(35)
H(5)	0796(8)	9457(28)	1895(5)	501(35)
H(6)	1615(10)	9844(20)	2763(13)	501(35)
H(7)	2735(4)	1142(3)	6912(2)	501(35)
H(8)	3540(4)	0730(3)	7862(2)	501(35)
H(9)	3494(4)	9881(3)	1803(2)	501(35)
H(10)	3212(4)	8333(3)	1705(2)	501(35)
H(11)	5310(4)	0394(4)	6732(2)	501(35)
H(12)	5637(4)	1940(4)	6810(2)	501(35)

Note. U_{eq} is defined as one-third of the tyrace of the orthogonalized U_{ij} tensor. The table of U_{ij} can be obtained upon request.

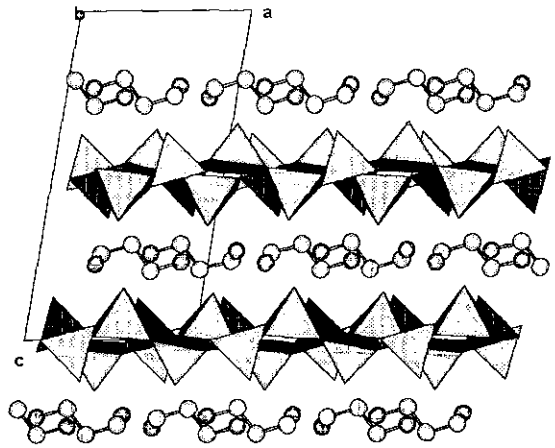

FIG. 1. (010) projection of $(VO)VO_4\cdot 0.5\ H_3N(CH_2)_3NH_3$ showing the two-dimensional character of the structure.

while the fourth is longer (1.837 Å) since the corresponding vertex is shared with two square pyramids. This remark will be of interest during the discussion of the structural relations. The bond valence analysis (25) clearly shows that the square pyramids are occupied by V^{4+} ions, and the tetrahedra by V^{5+}, therefore leading to a mixed valence compound of class I (26), with localized electrons.

Each polyhedron has a terminal oxygen; the others are shared between two or three polyhedra. Two square pyramids share an edge in such a way that in one pyramid the terminal oxygen is above the plane formed by the equatorial oxygens and below it in the second one. In the following, these two different positions will be labeled "up" and "down," for the pyramids and the tetrahedra, as well. These isolated double square pyramids (hereafter denoted DSQ) are linked together by tetrahedra, to form

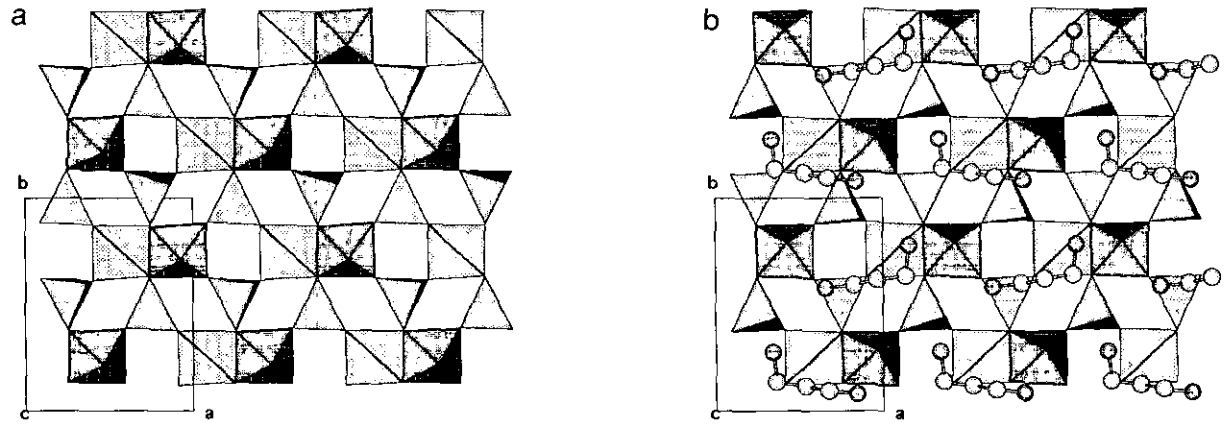

FIG. 2. (001) projection of the structure of $(VO)VO_4\cdot 0.5\ H_3N(CH_2)_3NH_3$ at $z = 0$ (a) and $z = 1/2$ (b). This shows the difference between the two layers where the DSQ are shifted from $a/2$, and the up and down orientation of the tetrahedra inverted between two planes. (b) The location of the amines toward the inorganic layer.

TABLE 3
Selected Distances (Å) and Angles (°) in $VO(VO_4)\cdot 0.5[C_3N_2H_{12}]$

V1	O2	O4	O3	O10	O5
	V(1) square pyramid: ⟨V(1)–O⟩ = 1.884 Å				
O2	*1.609(2)*	2.814(3)	2.880(3)	2.900(2)	2.916(2)
O4	105.0(1)	*1.931(2)*	2.681(3)	3.742(3)	2.670(2)
O3	108.5(1)	87.9(1)	*1.932(2)*	2.720(2)	3.706(3)
O10	107.6(1)	146.7(1)	88.3(1)	*1.974(2)*	2.466(3)
O5	108.4(1)	108.4(1)	142.9(1)	77.3(1)	*1.976(2)*
V2	O9	O1	O8	O10	O5
	V(2) square pyramid: ⟨V(2)–O⟩ = 1.880 Å				
O9	*1.612(2)*	2.870(3)	2.817(3)	2.897(2)	2.875(2)
O1	108.6(1)	*1.917(2)*	2.661(3)	3.692(3)	2.732(2)
O8	104.9(1)	87.5(1)	*1.934(2)*	2.676(2)	3.754(3)
O10	107.6(1)	143.7(1)	86.6(1)	*1.969(2)*	2.466(3)
O5	106.3(1)	89.3(1)	148.0(1)	77.5(1)	*1.971(2)*
V3	O7	O1	O4	O5	
	V(3) tetrahedron: ⟨V(3)–O⟩ = 1.725 Å				
O7	*1.653(2)*	2.737(2)	2.786(2)	2.849(3)	
O1	109.5(1)	*1.697(2)*	2.747(2)	2.826(3)	
O4	111.6(1)	107.2(1)	*1.714(2)*	2.960(3)	
O5	109.3(1)	106.1(1)	112.9(1)	*1.837(2)*	
V4	O6	O3	O8	O10	
	V(4) tetrahedron: ⟨V(4)–O⟩ = 1.724 Å				
O6	*1.647(2)*	2.726(2)	2.773(2)	2.849(3)	
O3	109.2(1)	*1.695(2)*	2.765(2)	2.851(3)	
O8	111.0(1)	108.3(1)	*1.717(2)*	2.934(3)	
O10	109.5(1)	107.5(1)	111.2(1)	*1.838(2)*	

1,3-DAP molecule

C(1)–N(1): 1.491(4) C(2)–N(2): 1.476(4) C(1)–C(3): 1.538(5) C(2)–C(3): 1.511(4)
N(1)–C(1)–C(3): 111.3(3) N(2)–C(2)–C(3): 111.7(3) C(2)–C(3)–C(1): 111.1(3)

Hydrogen bonds

O(2)–H(4):	2.09(2)	O(9)–H(3):	1.95(2)
O(6)–H(1):	1.88(1)	O(6)–H(5):	2.10(2)
O(7)–H(6):	1.96(2)	O(7)–H(2):	2.00(1)

Note. The N–H and C–H distances were fixed at 0.89 and 0.97 Å during the refinement.

TABLE 4
Valence Bond Analysis of $(VO)VO_4\cdot 0.5\ H_3N(CH_2)_3NH_3$

	V1	V2	V3	V4	Σ	Σ
O1	—	0.70	1.33	—	—	2.03
O2	1.60	—	—	—	0.05	1.65
O3	0.67	—	—	1.34	—	2.01
O4	0.67	—	1.27	—	—	1.94
O5	0.60	0.60	0.91	—	—	2.11
O6	—	—	—	1.52	0.13	1.65
O7	—	—	1.50	—	0.12	1.62
O8	—	0.66	—	1.26	—	1.92
O9	—	1.60	—	—	0.07	1.67
O10	0.59	0.61	—	0.91	—	2.11
Σ	4.14	4.17	5.01	5.03		

Note. The results refer to the equation $s = \exp[(R_0 - d)/0.37]$ (25) with R_0 = 1.784 and 1.803 for V^{4+} and V^{5+}, respectively.

the sheet (Figs. 2a and 2b). Two tetrahedra, one up and the other down, share the two oxygens corresponding to the medium distances V^{5+}–O with two different DSQ, and let appear a square vacancy within the secondary building unit. The latter is formed by two tetrahedra and two square pyramids (Fig. 3). The last vertex of each tetrahedron is common with the edge shared between two pyramids, and ensures the two-dimensional inorganic network with the composition $(V_2O_5)^-$. Figures 2a and 2b show also that two layers are shifted by $a/2$, with symmetric orientations of the tetrahedra from one sheet to the other.

The amines are diprotonated. They lie at $z \approx 1/4$ and 3/4, and their skeleton is parallel to the direction of the layers. On one layer, the nitrogens project above the square and the rhombic vacancies; on the other layer, the nitrogens are above the square and the triangle of the down polyhe-

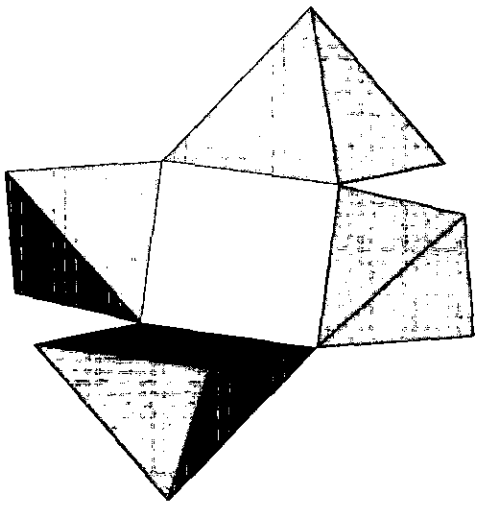

FIG. 3. Secondary building unit (SBU4) in $(VO)VO_4 \cdot 0.5\ H_3N(CH_2)_3NH_3$.

dra. The hydrogen of the amino groups give strong hydrogen bonds with the layer via the terminal oxygens of the pyramids and those of the tetrahedra which correspond to the shortest V–O bonds.

STRUCTURAL CORRELATIONS

Despite the originality of this structure, a type of layer closely related to ours was already encountered (Fig. 4) in the reduced cesium vanadate CsV_2O_5 (27). Its cell characteristics, labeled with C indices, are in close relations with those of this paper (V indices) [S. G. $P2_1/c$, a_c = 7.008 Å $\approx$ 1/2 c_v (interlayer space), b_c = 9.977 Å $\approx b_v$, c_c = 7.729 Å $\approx a_v$, β_c = 90.98°)], but with two important differences: (i) the up and down arrangement of the tetrahedra along the c_c axis is different, all up or all down in CsV_2O_5, and alternatively up and down in our case; (ii) all the sheets are identical and stacked one upon the other in CsV_2O_5, at variance to the $a/2$ shift and symmetrical position of the tetrahedra between two layers observed here. A similar arrangement of the planes is also encountered in the structure (28, 29) of vanadyl selenite $VOSeO_3$ [S.G. $P2_1/c$, a_s = 4.017 Å (interlayer space), b_s = 9.788 Å $\approx b_v$, c_s = 8.001 Å $\approx a_v$, β_c = 99.48°)], which does not have intercalated species between the layers. The VO_4 tetrahedra are replaced by the group SeO_3E, E being the lone pair on Se^{4+}. This structure will be discussed in more detail at the end of the paper, due to the lack of inserted particles in between the sheets.

Another related topology (Fig. 5) concerns $(VO)(HPO_4) \cdot 0.5\ H_2O$ (30, 31). Two of the three cell parameters, labeled with H indices, strongly differ from those of this paper (V indices) [S.G. *Pmmn*, a_H = 7.420 Å $< a_v$, b_H = 9.609 Å $\approx b_v$, c_H = 5.693 Å $\ll$ 1/2 a_v (interlayer space)]. These differences arise for two reasons: (i) in the layer, even if the tetrahedra have the same disposition as in the title compound, the decrease in a_H corresponds to the changes in the coordination polyhedra of V (octahedral with the sixth H_2O ligand instead of a square pyramid) and of their connection (faces instead of edges); (ii) there is no intercalated species between the stacked layers, and therefore, c_H is lowered, but not as much as for $VOSeO_3$, since the hydrogens of the water molecules which link the two octahedra point toward the interspace.

As the stoichiometry of the layer corresponds to the formula V_2O_5, the comparison between the topologies of the layers in the title compound and in the stable form of V_2O_5 (32 and references therein) is requested in order to find the relations between them. Whereas all the DSQ

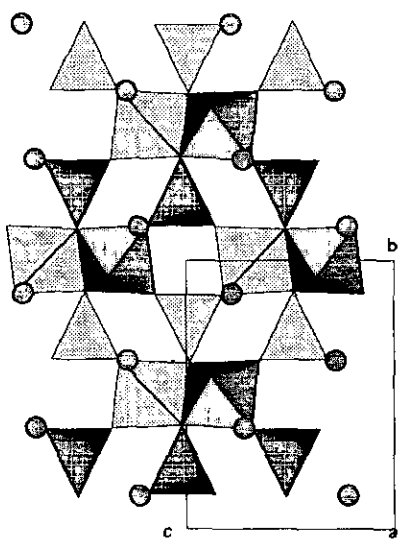

FIG. 4. Projection of CsV_2O_5 along [100]. Cs is represented by the circles.

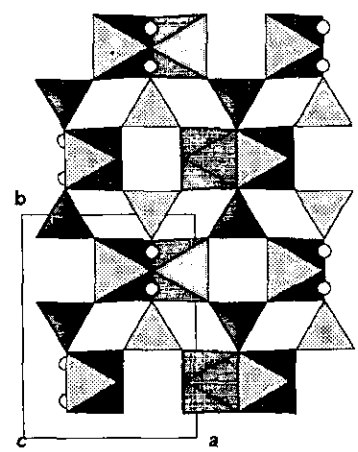

FIG. 5. Projection of the structure of $(VO)(HPO_4) \cdot 0.5\ H_2O$ along [001]. Small circles represent the hydrogens of the water molecule.

are oriented in the same way in $(VO)VO_4 \cdot 0.5$ DAP, the existence of double chains of pyramids with the same orientation in V_2O_5 leads to two symmetric orientations for the DSQ (Fig. 6a). Small displacements of some oxygens atoms (Fig. 6b) in the layer of V_2O_5, which might be induced by the presence of intercalated species, can transform it in a sheet in which all the DSQ have the same disposition, as is encountered (Fig. 6c) in the Mo partially substituted vanadium pentoxide $V_{2-x}Mo_xO_5$ ($x \approx 0.3$) studied by Khilborg (33). This modified form of V_2O_5 can be easily compared to the network of $(VO)VO_4 \cdot 0.5$ DAP (Fig. 7) if the former is not only described by square pyramids separated by square vacancies (Fig. 7b), but also by an alternation of rows of DSQ separated by vanadyl groups attached to the square vacancies of a row since this attachment corresponds to the V–O medium lengths as noted before (Fig. 7c). In this description, the equatorial oxygens of the sheet describe a 4^4 net according to the Schlafli symbolism (34). If each row shifts by half of the length of the edge of a pyramid (Figs. 7d and 7e), the 4^4 plane net of oxygens transforms into the 3^34^2 plane net, which exactly corresponds to the topology of $(VO)VO_4 \cdot 0.5$ DAP, thus illustrating the close relationship between the two structures. This mechanism of transformation, assuming that the vanadyl groups follow the vacancy during the shift, explains the change from square pyramidal to tetrahedral coordination for one-half of the vanadium between two M_2O_5 topologies.

At this stage of the discussion, another comparison must be made with the α-$VOPO_4$ network (35). It corresponds to another M_2O_5 topology (Fig. 8a) which, at variance to V_2O_5, keeps the same crystal chemistry when organic species are inserted in the interlayer space (36). The great difference between the two topologies, which are, however, built up from the same SBU (Figs. 8b and 8c), concerns the connectivity of the polyhedra. Single square pyramids exist in α-$VOPO_4$ whereas edge-shared double square pyramids appear in $VOVO_4$, the short V=O bonds being terminal in both cases. Moreover, the tetrahedra share all their vertices with single pyramids in α-$VOPO_4$ and have a terminal vertex in $VOVO_4$, the others being shared either with the two pyramids of the DSQ or with one of the pyramids of the DSQ. This implies many more constraints in α-$VOPO_4$, as can be seen in Table 5, which compares the characteristic angles and distances of the two SBU. An eventual transition between the two structure types would

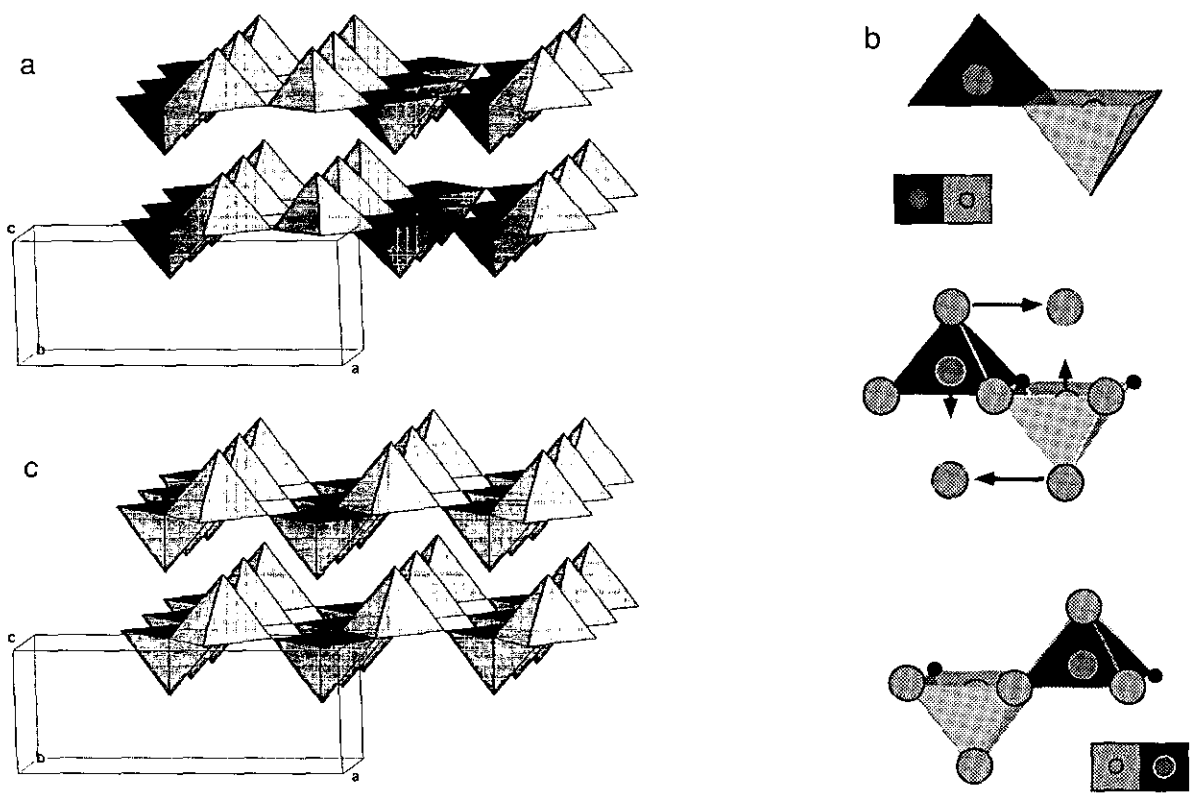

FIG. 6. (a) Perspective view of V_2O_5 with the symmetric double pyramids indicated by arrows, (b) atomic displacements which invert the disposition of the DSQ, and (c) perspective view of $V_{2-x}Mo_xO_5$, described in the same cell as V_2O_5, in which all the DSQ have the same orientation.

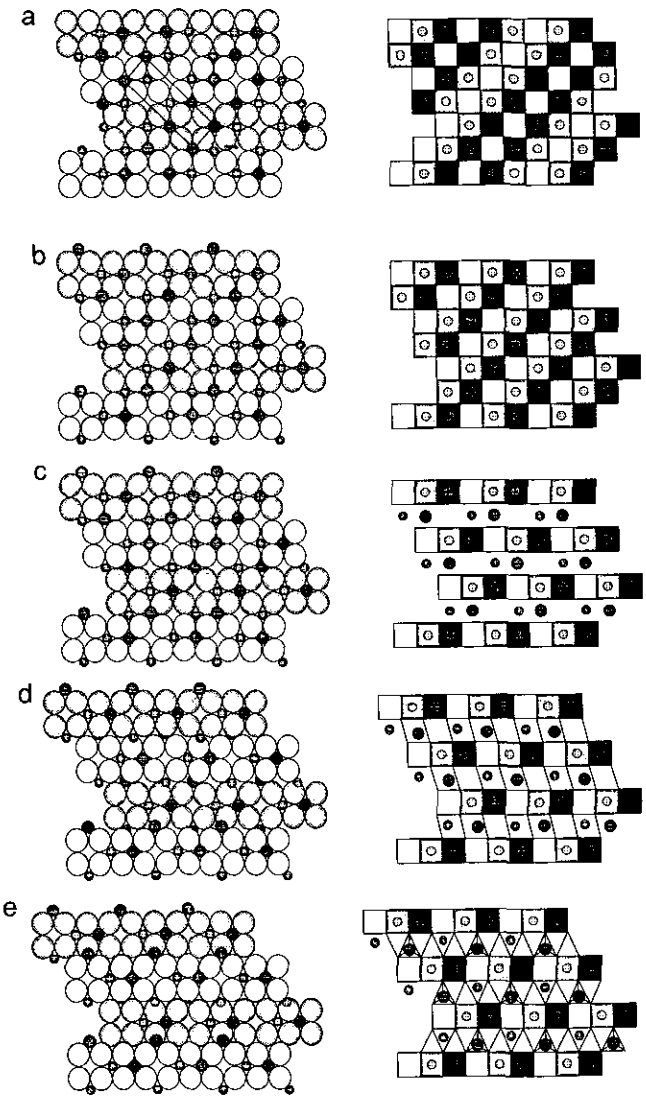

FIG. 7. Structural relationships between V_2O_5 and $(VO)VO_4 \cdot 0.5\ H_3N(CH_2)_3NH_3$ using spheres (left column) and polyhedra (right column) representation: (a) (001) projection of V_2O_5; dark and light squares correspond to up and down pyramids. (b) Projection after the displacements of Fig. 6b, leading to the $V_{2-x}Mo_xO_5$ form. (c) The same projection considering the solid as a succession of rows and vanadyl groups; large and small circles relate to up and down V=O bonds. (d, e) Shift by 1/4 (d) and 1/2 (e) edge of the pyramids to ensure the passage from V_2O_5 to $(VO)VO_4$ topology, and therefore from a fivefold to a tetrahedral coordination for the vanadium between the rows.

TABLE 5

Comparison of the Distortions of the Tetrametric Units in α-$(VO)PO_4$ and $(VO)VO_4 \cdot 0.5\ H_3N(CH_2)_3NH_3$

	α-$(VO)PO_4$	$(VO)VO_4$
V2(b–d)	144.36°	171.78°
T1(a–c)	154.99°	116.29°
O1–O2–O3	129.77°	157.09°
$\langle d_{V\text{-equatorial plane}} \rangle$	0.376 Å	0.577 Å

Note. Letters refer to those in Figs. 8b and 8c.

be exclusively reconstructive in each layer, with the break of two equatorial V–O bonds in the square pyramids, a rotation of the tetrahedra to create one terminal vertex, and a reorientation of the structural units formed from strong bonds, as indicated in Fig. 9.

As V_2O_5 and $VOPO_4$ are typically two-dimensional compounds with no intercalated species between the layers, a question arises now: what should be the structure of deintercalated vanadyl vanadate? Two possibilities may be inferred.

It may first be expected that, due to the close similarity between the topology of the layers of $VOSeO_3(E)$ (28, 29), already mentioned, and of the title compound, $VOVO_4$ would have the same arrangement of layers. However, in $VOSeO_3(E)$ all the layers are identical, with the tetrahedra oriented in the same way in two consecutive layers, whereas we previously noted that two layers in $(VO)VO_4 \cdot 0.5$ DAP are shifted by $a/2$, with symmetrical orientations of the tetrahedra. The transformation of the title compound into a new two-dimensional form of V_2O_5 (Fig. 10a) by deintercalation would then require the oxidization of V^{4+} into V^{5+}, an inversion of the orientation of the tetrahedra in one-half of the layers, and their $a/2$ shift to give the stacking observed in $VOSeO_3(E)$, and therefore an interlayer parameter close to 4 Å.

The other possibility of deintercalation, keeping this time the orientation of the tetrahedra in the layers, might lead to a three-dimensional compound after the $a/2$ shift. This might be done by condensation of two VO_4 tetrahedra into a pyrovanadate V_2O_7 group, with the oxygen being eliminated as water with the hydrogens which protonated the amines. The topology of the resulting compound $(VO)_2V_2O_7$, in which the mixed valence character of vanadium would be preserved, should be very close (Fig. 10b) to the well-known $(VO)_2P_2O_7$ (37). In such a hypothesis, the deintercalation should lead to a new form of V_4O_9.

MAGNETIC RESULTS

The thermal variation of the inverse susceptibility curve is given in Fig. 11. It clearly shows that the compound orders antiferromagnetically below 20(3) K. The characteristics of the curve are very closely related with those of Trombe *et al.* (29) on $VOSeO_3$. The explanation of the magnetic behavior proposed by the authors for the latter compound strictly apply to our case.

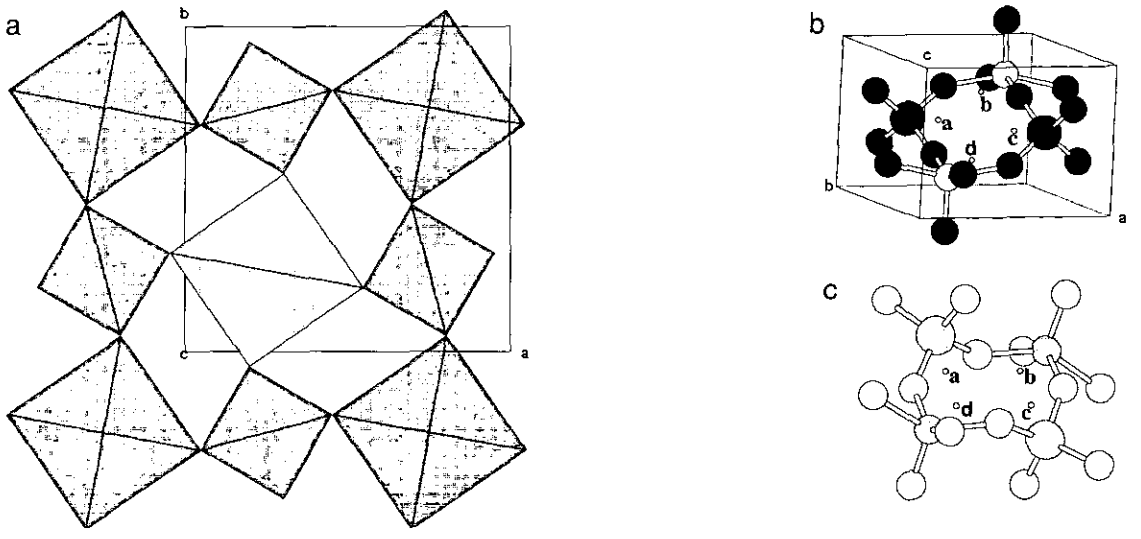

FIG. 8. (a) (001) projection of α-$VOPO_4$. (b) SBU of α-$VOPO_4$. (c) SBU of $VOVO_4$. In (b) and (c), small circles denoted a, b, c, d correspond to the middle of the edges of the polyhedra which determine the central vacancy.

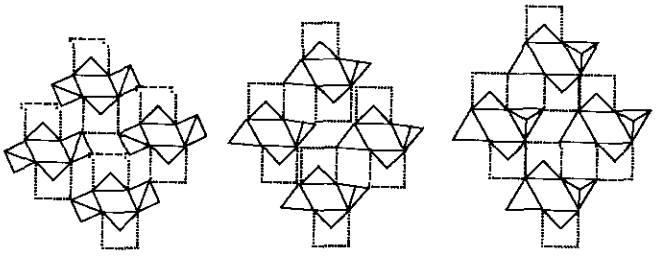

FIG. 9. A possible transformation of α-$VOPO_4$ (left) into $VOVO_4$ (right). The structural units are formed by two tetrahedra twice linked by two V–O strong bonds (rectangular triangles) of the square pyramid (always represented by dotted lines). The middle drawing indicates the rearrangement of the tetrameric units by rotation of the tetrahedra.

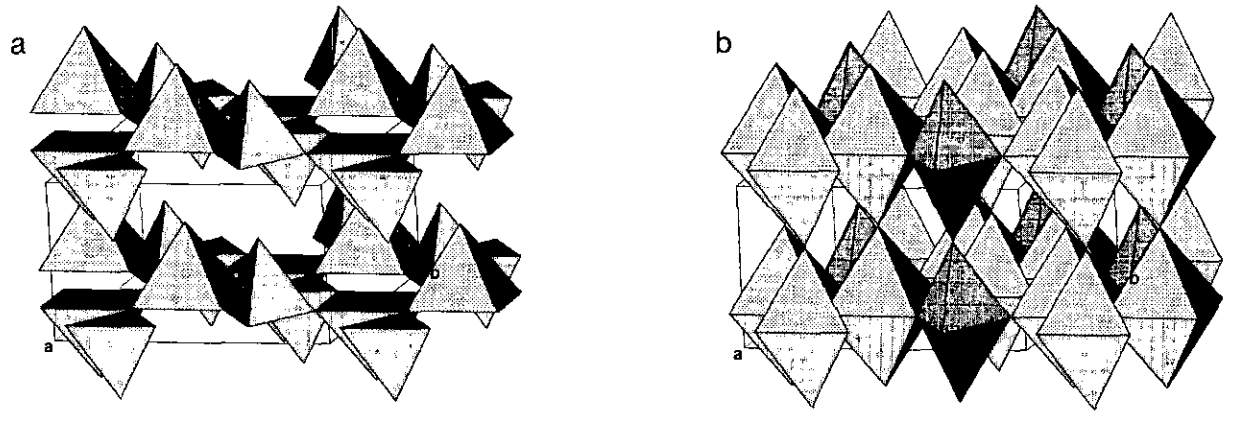

FIG. 10. (a) Hypothetical new form of V_2O_5 with vanadium in tetrahedral and square pyramidal coordination. (b) Hypothetical new form of V_4O_9 with close relations with the $(VO)_2P_2O_7$ structure.

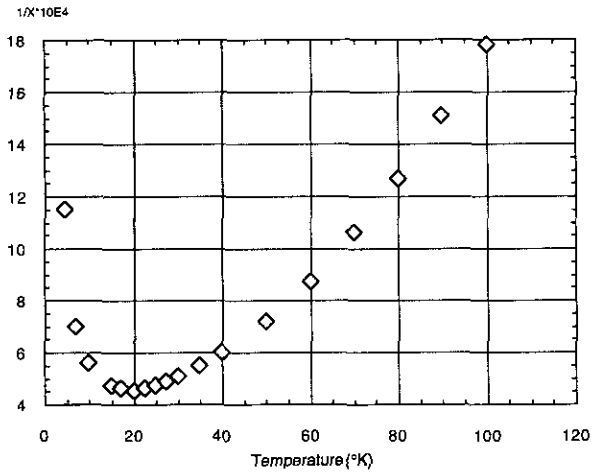

FIG. 11. Thermal variation of the inverse of the magnetic susceptibility (per g) for $(VO)VO_4 \cdot 0.5$ DAP.

ACKNOWLEDGMENTS

The authors are indebted to Dr. R. Retoux (Université du Maine) for his help in the data collection, and to Dr. J. Galy (CEMES, Toulouse) for helpful discussions.

REFERENCES

1. J. L. Guth, H. Kessler, and R. Wey, *Stud. Surf. Sci. Catal.* **28,** 121 (1986).
2. J. L. Guth, H. Kessler, J. M. Higel, J. M. Lamblin, J. Patarin, A. Seive, J. M. Chezeau, and R. Wey, *ACS Symp. Ser.* **398** 176 (1989).
3. H. Kessler, *Mater. Res. Soc. Symp. Proc.* **233,** 47 (1991).
4. M. Estermann, L. B. McCusker, C. Baerlocher, A. Merrouche, and H. Kessler, *Nature* **352,** 320 (1991).
5. T. Loiseau and G. Férey, *J. Chem. Soc. Chem. Commun.* 1197 (1992).
6. T. Loiseau and G. Férey, *Eur. J. Solid State Inorg. Chem.* **30,** 369 (1993).
7. G. Férey, T. Loiseau, P. Lacorre, and F. Taulelle, *J. Solid State Chem.* **105,** 179 (1993).
8. F. Taulelle, T. Loiseau, J. Maquet, J. Livage, and G. Férey, *J. Solid State Chem.* **105,** 191 (1993).
9. G. Férey, T. Loiseau, and D. Riou, *Mater. Sci. Forum* **152/153,** 125 (1994).
10. T. Loiseau, D. Riou, and G. Férey, *Stud. Surf. Sci. Catal.* **84,** 135 (1994).
11. T. Loiseau and G. Férey, *J. Solid State Chem.* **111,** 397 (1994).
12. T. Loiseau, R. Retoux, P. Lacorre, and G. Férey, *J. Solid State Chem.* **111,** 427 (1994).
13. M. Cavellec, D. Riou, and G. Férey, *Eur. J. Solid State Inorg. Chem.* **31,** 583 (1994).
14. F. Serpaggi, T. Loiseau, D. Riou, M. W. Hosseini, and G. Férey, *Eur. J. Solid State Inorg. Chem.* **31,** 595 (1994).
15. D. Riou and G. Férey, *Eur. J. Solid State Inorg. Chem.* **31,** 605 (1994).
16. V. Soghomonian, Q. Chen, R. C. Haushalter, J. Zubieta, and C. J. O'Connor, *Science* **259,** 1509 (1993).
17. V. Soghomonian, Q. Chen, R. C. Haushalter, and J. Zubieta, *Angew. Chem. Int. Ed. Engl.* **32**(4), 610 (1993).
18. T. Loiseau and G. Férey, *J. Solid State Chem.* **111,** 416 (1994).
19. D. Riou and G. Férey, *J. Solid State Chem.* **111,** 422 (1994).
20. D. Riou, M. Cavellec, and G. Férey, *Acta Crystallogr. Sect. C* **50,** 1379 (1994).
21. M. Cavellec, D. Riou, and G. Férey, *J. Solid State Chem.* **112,** 441 (1994).
22. "International Tables for X-ray Crystallography." Kluwer Academic, Dortrecht, 1984.
23. G. M. Sheldrick, *Acta Crystallogr. Sect. A* **46,** 467 (1990).
24. G. M. Sheldrick, SHELXL-93, A Program for Crystal Structure Determination, University of Göttingen, Germany, 1993.
25. N. Brese and M. O'Keeffe, *Acta Crystallogr. Sect. B* **47,** 192 (1991).
26. M. B. Robin and P. Day, *Adv. Inorg. Chem. Radiochem.* **10,** 247 (1967).
27. W. G. Mumme and J. A. Watts, *J. Solid State Chem.* **3,** 319 (1971).
28. J. C. Trombe, R. Enjalbert A. Gleizes, and J. Galy, *C.R. Acad. Sci. Ser. II* **297,** 667 (1983).
29. J. C. Trombe, A. Gleizes, J. Galy, J. P. Renard, Y. Journaux, and M. Verdaguer, *New J. Chem.* **11**(4), 321 (1987).
30. C. C. Torardi and J. C. Calabrese, *Inorg. Chem.* **23,** 1308 (1984).
31. M. E. Leonowicz, J. W. Johnson, J. F. Brody, H. F. Shannon, and J. M. Newsam, *J. Solid State Chem.* **56,** 370 (1985).
32. R. Enjalbert and J. Galy, *Acta Crystallogr. Sect. C* **42,** 1467 (1986).
33. L. Khilborg, *Acta Chem. Scand.* **21,** 2495 (1967).
34. M. O'Keeffe and B. Hyde, *Philos. Trans. R. Soc. London A* **295,** 553 (1980).
35. B. Jordan and C. Calvo, *Can. J. Chem.* **51,** 2621 (1973).
36. D. Riou and G. Férey, *Eur. J. Solid State Inorg. Chem.* **31,** 25 (1994).
37. P. T. Nguyen, R. D. Hoffman, and A. W. Sleight, *Mater. Res. Bull.* **30**(9), 1055 (1995).